Identification and Characterization of Novel Small Molecules as Potent Inhibitors of the Plasmodial Calcium-Dependent Protein Kinase 1[†]

Guillaume Lemercier,[‡] Amaury Fernandez-Montalvan,[‡] Jeffrey P. Shaw,[‡] Dominik Kugelstadt,[§] Joerg Bomke,[‡] Mathias Domostoj,[‡] Matthias K. Schwarz,[‡] Alexander Scheer,[‡] Barbara Kappes,[§] and Didier Leroy*,[‡]

[‡]*Geneva Research Center, Merck-Serono SA, 9, chemin des Mines, Case postale 54CH-1211 Genève 20, Switzerland, and* [§]*Institute of Hygiene, Department of Parasitology, University of Heidelberg, Im Neuenheimer Feld 324, 69120 Heidelberg, Germany*

Received March 25, 2009; Revised Manuscript Received June 3, 2009

ABSTRACT: Malaria remains a major killer in many parts of the world. Recently, there has been an increase in the role of public−private partnerships inciting academic and industrial scientists to merge their expertise in drug-target validation and in the early stage of drug discovery to identify potential new medicines. There is a need to identify and characterize new molecules showing high efficacy, low toxicity with low propensity to induce resistance in the parasite. In this context, we have studied the structural requirements of the inhibition of *Pf*CDPK1. This is a calcium-dependent protein kinase expressed in *Plasmodium falciparum*, which has been genetically confirmed as essential for survival. A primary screening assay has been developed. A total of 54000 compounds were tested, yielding two distinct chemical series of nanomolar small molecule inhibitors. The most potent members of each series were further characterized through enzymatic and biophysical analyses. Dissociation rates of the inhibitor−kinase complexes were shown to be key parameters to differentiate both series. Finally, a homology-based model of the kinase core domain has been built which allows rational design of the next generation of inhibitors.

Malaria is the most deadly tropical disease. It affects up to three hundred million people yearly, causing the death of almost a million of them, the vast majority are children in sub-Saharan Africa. The emergence of parasitic strains resistant to classical drugs used currently in chemotherapeutic treatments means that these are no longer recommended therapy in disease endemic countries (*1−5*). Artemisinin combination therapies (ACTs) have become the standard course of treatment (*6*), but given the potential of artemsinin resistance developing, there is clearly a need for new generations of molecules.

Nowadays, the discovery of new antimalarial medicines is entering a new era. Indeed, the access to hit/lead identification processes of several pharmaceutical industries opened new opportunities for the malaria research community. Moreover, the sequencing of the whole genome of *Plasmodium falciparum* (*Pf*)[1] revealed a substantial number of genes whose products represent a source of potential targets for the discovery of new antimalarial drugs. The divergence observed between protein kinases from *Plasmodium* and their human homologues suggests that the specific inhibition of a parasitic pool of these enzymes is achievable (*7−11*). Moreover, molecular mechanisms that control parasite invasion, proliferation, and viability (*12−17*)

have been shown to rely on protein kinases as demonstrated by various reverse genetic-based studies (*18−21*).

Calcium-dependent protein kinases belong to a well-defined gene product family found in plants and Alveolates but not in man (*22*). Five genes encoding five CDPKs (*Pf*CDPK 1−5), have been identified in the genome of *P. falciparum* (*23−27*). Amino acid identity among paralogues within the CDPK family is 39−56%. The calmodulin-independent property of these protein kinases is supported by a protein architecture where a highly conserved N-terminal serine/threonine protein kinase domain is contiguous with a C-terminal domain made of four EF-hand calcium binding motifs. While the functions of *Pf*CDPK2 and *Pf*CDPK5 are unknown, *Pf*CDPK1 is a calcium-dependent calmodulin-independent protein kinase (*28*) expressed during the whole intraerythrocytic stage of the parasite and is associated with membranes and organelle fractions (*29, 30*). Accumulation of *Pf*CDPK1 in specific intracellular compartments of the parasite suggests its involvement in active membrane biogenesis of blood stage parasites and also in the mechanism of merozoite invasion. Despite several attempts, it has not been possible to knockout the gene encoding for CDPK1 in *P. falciparum* parasites ((*31*); B. Kappes, unpublished data), suggesting that this enzyme is essential for parasitic viability. The recent pharmacological validation of CDPK1 essentiality in *P. falciparum* has raised interest in designing potent inhibitors of this enzyme with antimalarial properties (*31*).

In the present study, we have identified tools to inhibit *Pf*CDPK1, assessed their mode of inhibition, and determined their interaction with this plasmodial protein kinase. First, the

[1]Abbreviations: ATP, adenosine triphosphate; BSA, bovine serum albumin; CDPK, calcium-dependent protein kinase; *Cp*, *Cryptosporidium parvum*; DMSO, dimethyl sulfoxide; HTS, high-throughput screening; *Pf*, *Plasmodium falciparum*; SAR, structure−activity relationships; SPR, surface plasmon resonance.

enzymatic parameters of the kinase reaction were determined, and a robust assay measuring ATP consumption was developed that proved suitable for HTS. Second, a detailed analysis of the mechanism of inhibition of two different series of small molecules was completed to identify potent inhibitors that could be optimized to the status of lead compound through further *in vitro* and *in vivo* studies. The access to biophysical interaction parameters was seen as a key factor for the design of new inhibitors on the basis of structure−activity relationships (SAR). The identification of new chemical series with unprecedented description of their mode of interaction constitutes a solid starting point for a drug discovery program.

EXPERIMENTAL PROCEDURES

Materials. Unless otherwise indicated, chemicals were purchased from Sigma-Fluka (St. Louis, MO). [γ-^{33}P]ATP (specific activity 2500 Ci/mmol) was from Amersham Biosciences (Little Chalfont, U.K.). Nonbinding surface (NBS) 96- and 384-well plates were from Corning Inc. (Corning, NY). The reference compound staurosporine was purchased from Alexis (Lausen, Switzerland). PK light HTS kinase assay kits were purchased from Cambrex/Lonza Biosciences (Basel, Switzerland). Biacore S51, CM5 series sensor chips, and coupling reagents (*N*-ethyl-*N'*-(3-dimethylaminopropyl)carbodiimide (EDC), *N*-hydroxysuccinimide (NHS), and ethanolamine hydrochloride) were purchased from Biacore AB.

Expression and Purification of PfCDPK1. His-tagged *Pf*CDPK1 was expressed in the *E. coli* strain BL21(DE3)pLys from the plasmid pET21a following induction by isopropyl 1-thio-β-galactopyranoside (IPTG) (*23*). Cells from a 10 L culture were harvested by centrifugation and washed once in cold buffer A (50 mM Tris-HCl, pH 7.5, 300 mM NaCl) containing 10% glycerol. The washed pellet was kept overnight at −20 °C. All following steps were carried out at 4 °C except where indicated. The frozen pellets were thawed and resuspended in buffer A (5 mL/g) containing 10% glycerol, protease inhibitors (1 mM phenylmethanesulfonyl fluoride, 20 μg/mL soybean trypsin inhibitor, 1 μg/mL pepstatin A, 10 μg/mL leupeptin), 0.3% Triton X-100, and 1 mg/mL lysozyme and incubated for 20 min at room temperature. The suspension was disrupted by sonication 5 times for 15 s each time. DNase I was added to a final concentration of 10 μg/mL. After incubation for 20 min, the suspension was cleared by centrifugation at 30000*g* for 30 min. The crude supernatant was adjusted to a imidazole concentration of 20 mM and applied to a 1.5 × 10 cm column of nickel-NTA agarose (Qiagen) preequilibrated with 20 mM imidazole in buffer A. The column was washed with 100 mL of the equilibration buffer followed by 200 mL of buffer A containing 33 mM imidazole. The kinase was eventually eluted with buffer A containing 100 mM imidazole. Fractions containing kinase activity were pooled. The pool was concentrated and subsequently chromatographed on a Sephacryl S-300 column (2.6 × 86 cm) preequilibrated in buffer A. The flow rate was approximately 16−18 mL/h. For storage, glycerol was added to a final concentration of 10%, and the protein was frozen at −80 °C.

Filtration Assay. In a NBS 96-well plate, 10 μL of compound at 50 μM diluted in 5% DMSO was incubated with 20 μL of enzyme (80 ng per well) and 20 μL of a mixture of ATP (20 μM), substrate (20 μM of casein or histone), and [γ-^{33}P]ATP (1 μCi per well). Solutions were prepared in a 50 mM Tris-HCl (pH 7.4) buffer containing MgCl$_2$ (10 mM), CaCl$_2$ (1.0 mM), Na$_3$VO$_4$ (100 μM), and dithiothreitol (0.5 mM). The incubation was stopped after 1 h by the addition of 50 μL of stop solution (saturated EDTA, 5 mM, and BSA, 1 mg/mL). After incubation for 15 min, the assay volume was transferred onto a filter plate, filtered on a multiscreen vacuum manifold (Millipore Corp., Billerica, MA), and washed extensively with wash buffer containing 50% ethanol/49% H$_2$O/1% orthophosphoric acid. Scintillation cocktail (100 μL) was then added and incubated for 2 h before the detection of the amount of radioactivity with a Trilux scintillation counter (Perkin-Elmer Life Sciences, Schwerzenbach, Switzerland).

Chemiluminescent Assay. Either 5 μL of compounds, selected as a library subset of 50000 molecules, a majority of which bearing protein kinase inhibitor scaffolds and dissolved in 5% DMSO, or 5 μL of 5% DMSO was incubated with 10 μL of substrate (casein, 0.9 mg/mL, and ATP, 10 μM, final concentrations) in a black NBS 384-well plate. Ten microliters of enzyme (25 ng per well) was added to start the reaction. Substrates and enzyme were diluted in a buffer containing 20 mM Tris-HCl, 0.5 mM DTT, 10 mM MgCl$_2$, and 1 mM CaCl$_2$. Plates were incubated at 30 °C for 2 h. The kinase reaction was stopped by addition of 5 μL of PK light stop solution, and 10 μL of PK light ATP detection reagent was added. The plates were incubated at room temperature for 1 h, and the luminescence was detected using a Victor2 V reader (Perkin-Elmer Life Sciences).

Calculation and Data Analysis. K_m and V_{max} values were calculated using Prism software (Graphpad Software Inc., San Diego, CA). Screening data were treated with the Genedata Screener Assay analyzer software (Genedata AG, Basel, Switzerland) and IC$_{50}$ values determined using Genedata Screener Condoseo software. Percentage of inhibition was calculated using Genedata from the difference between the average signal of the controls providing high chemiluminescence intensity (no enzyme; ATP concentration and signal are maximum) and the average signal of the controls providing low chemiluminescence intensity (with enzyme but without inhibitors; ATP concentration and signal are minimum). This difference represents 100% of activity.

To evaluate the quality of assays, robustness was assessed by calculating the signal to background ratio and the Z' factor value (*32*) using the equation: $Z' = 1 - ((3\text{SD of high intensity control}) + (3\text{SD of low intensity control}))/|(\text{mean of high intensity control} - \text{mean of low intensity control})|$.

Biacore-Based Analysis of Interaction Parameters. (A) PfCDPK1 Immobilization. *Pf*CDPK1 was immobilized onto CM5 (series S) sensor chips using standard amine coupling. HBS-P, which consisted of 10 mM Hepes, pH 7.4, 0.3 M NaCl, and 0.005% P20, was used as a running buffer. The carboxymethyldextran surface within one side of the flow cell was activated with a 7 min injection of a 1:1 ratio of 0.4 M EDC and 0.1 M NHS. The enzyme was coupled to the surface with a 10 min injection of *Pf*CDPK1 diluted to 50 μg/mL in 20 mM BisTris, pH 6.0, with either 0.5 mM ATP/MgCl$_2$ or 2 μM AS275539 at a flow rate of 10 μL/min. Remaining activated groups were blocked with a 7 min injection of 1.0 M ethanolamine, pH 8.5. Typically 15000 ± 2000 RU's of *Pf*CDPK1 were immobilized for the different experiments described under Results.

(B) Binding Experiments. Compounds stored as 10 mM stock solutions in 100% dimethyl sulfoxide (DMSO) were dissolved directly in running buffer (20 mM Tris-HCl, pH 7.4, 50 mM NaCl, 10 mM MgCl$_2$, 0.5 mM CaCl$_2$, 0.05% P20, 1 mM DTT, 2% DMSO) and analyzed with a Biacore S51 using a 2-fold dilution series. The highest compound concentration varied, but all compounds were tested at 10 different concentrations, and

each concentration was tested at least five times. Interaction analysis cycles consisted of a 60 s sample injection (30 μL/min) followed by 300 s of buffer flow (dissociation phase). All of the bound complexes dissociated back to baseline within a reasonable time frame, and regeneration was required.

(C) Data Processing and Fitting. All sensorgrams were processed by first subtracting the binding response recorded from the control surface (center reference spot), followed by subtracting an average of the buffer blank injections from the reaction spot (*33*). To determine kinetic rate constants, all data sets were fit to a simple 1:1 interaction model including a term for mass transport using numerical integration and nonlinear curve fitting (*33*). Equilibrium analysis was performed by fitting the response at the end of the association phase to a single-site binding isotherm.

Molecular Modeling. The amino acid sequence of *Pf*CDPK1 was compared and aligned to those of all entries comprising the protein structure database (www.rcsb.org), and the results of the comparison and alignment were examined manually. Notably, the amino acid sequence of the entry 2qg5, which corresponds to a calcium calmodulin-dependent protein kinase of *Cryptosporidium parvum* (Lunin, V. V., Wernimont, A. K., Lew, J., Wasney, G., Kozieradzki, I., Vedadi, M., Bochkarev, A., Arrowsmith, C. H., Sundstrom, M., Weigelt, J., Edwards, A. E., Hui, R., Artz, J., and Amani, M., *Cryptosporidium parvum* calcium dependent protein kinase cgd7_1840, to be published), another apicomplexan parasite, had 37% identity with the sequence of *Pf*CDPK1 in the region including the kinase domain. A 410 amino acid overlap exists between the two structures including residues 47−346 of *Pf*CDPK1 and residues 197−457 of the *C. parvum* protein kinase (Figure 6A). A close manual inspection of the amino acid content of the ATP-binding motif between the *P. falciparum* CDPK1 and the *C. parvum* CDPK revealed very few significant differences, and the latter was thus used as the protein template for docking experiments without any modifications, except for those produced by the protein preparation workflow in the Schrodinger software package Maestro (which consists of protonation of the otherwise unaltered protein structure and optimization of any internal hydrogen-bonding networks). The identification of the putative binding mode of two molecules, 2-amino-3-[(4-methylphenyl)carbonyl]indolizine-1-carboxamide and imidazo[1,2-β]pyridazine, into the active site of *Cp*CDPK was performed using the program Glide (*34*) with the default parameters. The active site of *Cp*CDPK was identified as a 15 Å cube centered on the peptide bond of the hinge region proton donor (Leu282). The various conformers of compounds **1** and **2** were produced by the program Ligprep using the default parameters. For the actual docking, the resulting poses were required to satisfy the formation of a hydrogen bond interaction between the peptide bond nitrogen of Glu281 as donor and the small molecule as acceptor.

RESULTS

Enzymatic Parameters of PfCDPK1. The success of target-based drug discovery is highly dependent on an accurate enzymatic characterization of the target of interest. *Pf*CDPK1 is a peculiar protein kinase in which optimal conformation is tightly regulated by calcium and impacts directly on the catalytic activity. The kinetic parameters of the kinase were determined according to "Michaelis−Menten" conditions with a standard radioactive filtration assay. Maximal velocity (V_{max}) and K_m value for ATP were found to be 60 nmol min^{-1} mg^{-1} and 40 μM,

respectively (Figure 1A). This is in accordance with the 70 nmol min^{-1} mg^{-1} and 26 μM values previously published (*29*). Size, isoelectric point, and amphiphilicity of substrates are known to potentially influence enzymatic efficacy through protein conformation changes, and those parameters may impact on the chemical diversity of small molecules identified as protein kinase inhibitors. Therefore, in order to study the influence of the net charge of protein substrates on the catalysis efficiency of *Pf*CDPK1, we analyzed the phosphorylation level of acidic proteins (casein and dephosphorylated casein) and basic proteins (histones H1, H2 and H3). *Pf*CDPK1 phosphorylated β-casein and histone H3 preferentially compared to histone H1, histone H2, and dephosphorylated casein (Figure 1B). Consequently, casein was the substrate that was selected for the following studies and the hit discovery phase. For casein, a K_m value of 0.16 mg/mL corresponding to 6.6 μM was determined (Figure 1C). The dependency of *Pf*CDPK1 in calcium ions was measured with the filtration assay, and the half-maximal activity (EC$_{50}$) was reached for a Ca^{2+} concentration of 18.6 μM (Figure 1D), a value which is close to the published one (15 μM). On the whole, the enzymatic parameters of *Pf*CDPK1 that we measured were close to the values published previously, confirming that the enzyme dedicated to the hit discovery phase had all of the quality criteria requested to finalize assay development and enable the identification of effective molecules.

Optimization of Assay Conditions. First, assay conditions were defined using a standard radioactive filtration-based assay with buffer characteristics described by Zhao et al. (*29*). Given that detergents prevent protein clogging and nonspecific binding, the influence of Triton X-100, Igepal, and Brij-35%, three nonionic detergents, was evaluated at different concentrations. We observed that the presence of these detergents in the assay was detrimental to *Pf*CDPK1 catalysis (Figure 2A), 0.01% being sufficient to decrease the enzymatic activity by at least 35% as compared to detergent-free conditions. The assay was also sensitive to Tween 20, yet to a lesser extent. At this point, it was decided that further optimizations of the assay should be performed in the absence of detergent. Tolerance of the assay to DMSO is another important parameter that needed to be assessed. Up to 2%, DMSO did not affect *Pf*CDPK1 activity significantly, and therefore, in the assay the final concentration of this solvent was set at 1% (Figure 2B). To accommodate the high number of compounds to be tested in HTS format, assay development was pursued with a homogeneous nonradioactive technology relying on bioluminescence-based measurement of ATP consumption. Signal intensity, ATP conversion (%), and assay robustness (Z' factor) were considered to adapt the assay to a suitable screening format. Thus, several conditions such as concentrations of enzyme and substrate, interruption of the enzymatic reaction, volume of the detection reagent, and incubation time were tested with the purpose of optimizing the assay. The addition of reagents was then automated in a 384-well format. The following conditions were chosen as a good compromise between robustness, signal window, and enzyme consumption: 0.9 mg/mL casein (37 μM), 10 μM ATP, 1.0 mM CaCl$_2$, 25 ng of enzyme per well (16.5 nM), and 1% DMSO, in a final volume of 25 μL. In these conditions, the enzyme activity was linear during 3 h at 30 °C. While the signal was stable during 4 h after the reaction had been stopped, the plates were read 1 h after the addition of the detection solution, when the signal intensity was maximal. PK light reagents measure nonhydrolyzed ATP after a given reaction time, and the use of an ATP
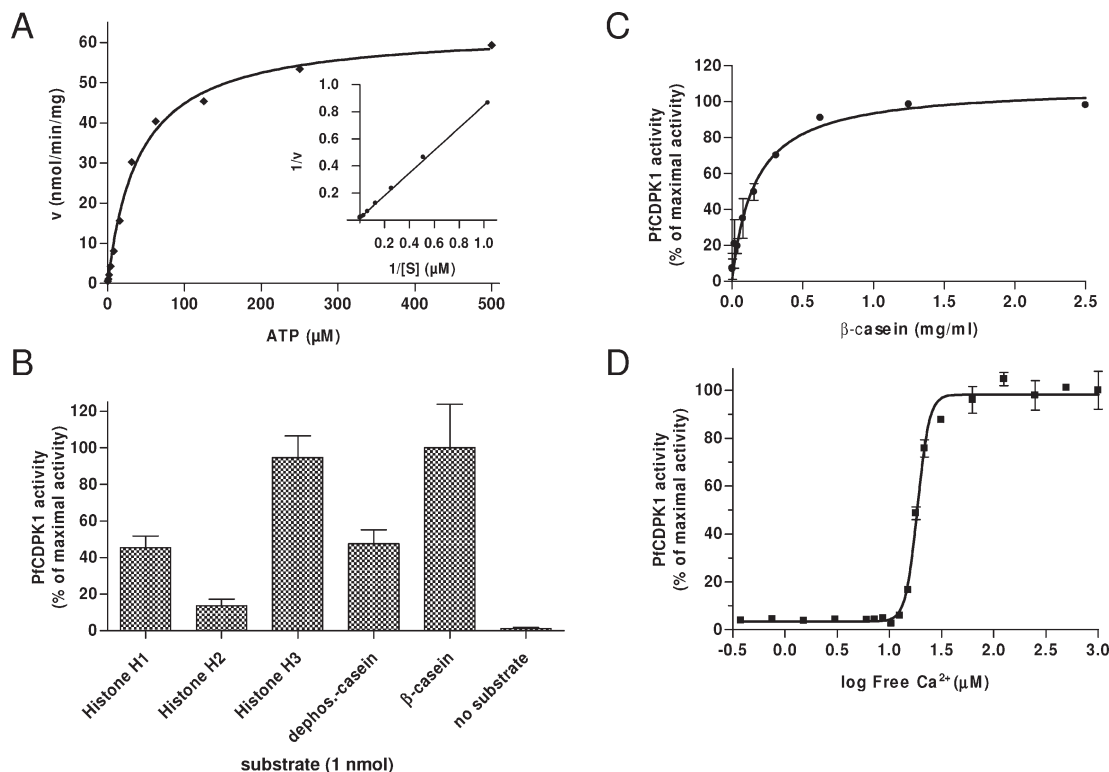
FIGURE 1: Enzymatic characterization of *Pf*CDPK1. (A) Apparent affinity of ATP. Activity of the recombinant enzyme was determined by a radioactive filtration assay. *Pf*CDPK1 was incubated with increasing concentrations of $[\gamma\text{-}^{33}\text{P}]$ATP and 0.9 mg/mL β-casein, 10 mM $MgCl_2$, 1 mM $CaCl_2$, and 0.5 mM DTT at pH 7.5 for 30 min. The inset is the representation of the data according to Lineweaver−Burk. (B) *Pf*CDPK1 substrate specificity was evaluated with various exogenous kinase substrates (1 nmol). Maximal activity (100%) corresponds to the activity observed with β-casein in the standard conditions (described in (A)). (C) Apparent affinity of β-casein. Enzymatic activity was determined in the presence of increasing concentrations of β-casein and 200 μM ATP in the standard conditions (described in (A)). (D) Calcium-mediated activation of *Pf*CDPK1. The concentration of free calcium varied by addition of $CaCl_2$ in the presence of 15 mM EGTA. EGTA was added to counterbalance the observed Ca^{2+} contamination in the buffer, and free Ca^{2+} concentration was calculated using the WinMaxC software taking into account the concentration of Mg^{2+}, contaminating Ca^{2+}, $CaCl_2$, ATP, and EGTA.

concentration above 20 μM was proven detrimental to the detection window. Consequently, the screen was performed with 10 μM ATP, a concentration much below the K_m value of ATP (40 μM). Staurosporine, a well-known pan-selective kinase inhibitor, was used as control inhibitor and was added to each plate at two different concentrations, 8 nM and 2 μM, leading to nearly 50% and 100% inhibition, respectively.

Hit Discovery. Benefiting from optimized assay conditions, 54733 compounds selected from the proprietary compound library were tested at a concentration of 10 μM. The first 9878 compounds were analyzed in duplicate to assess the reproducibility of the assay in the presence of inhibitors (Figure 3A). The good correlation between the two independent series of data, the high robustness of the assay, and the strong statistics provided by this set of molecules allowed the hit discovery phase to be pursued in a simplicate mode (Figure 3). The entire screen was performed with the lot of enzyme that has been used during assay development. Within the whole screen, the average standard deviation of the signal without inhibitor was 4.4% (1−9.7%), whereas the standard deviation of the signal without enzyme was 5.2% (1.61−7.6%). The average signal to background ratio was 11 with a standard deviation of 5.7, yet those variations had no strong influence on the averaged Z factor value, which was found to be 0.75 with a standard deviation of 0.1. Indeed, the lowest signal to background ratio of 2.6 led to a decent robustness (Z factor > 0.68; data not shown). Considering a threshold of 50% inhibition (more than 9-fold the standard deviation from signal without enzyme), 265 compounds defined as "hits" were

identified (hit rate = 0.48%). Hit compounds were tested in triplicate at a concentration of 10 μM. The occurrence of false positives was less than 3%. Inhibitory concentrations at 50% (IC_{50}) of the most potent compounds were estimated using dose response curves from three independent experiments, and so far, 70 compounds with submicromolar activities were identified. The quality of the most potent compounds was controlled by liquid chromatography/mass spectrometry analysis as described by Pomel and co-workers (*35*). All of the compounds tested had purity greater than 95% and for most of them even greater than 99%. In a second step, the most potent compounds were either ordered again from the supplier or synthesized in-house, and the potency of each new batch of molecules was analyzed. No significant difference was observed between the IC_{50} values from different lots of the same molecules.

Kinase Selectivity of the Inhibitors. The selectivity of four inhibitors was evaluated at a concentration of 10 μM against a panel of 46 human protein kinases (Millipore, U.K.; details of the experimental procedure are available at http://www.millipore.com/techpublications/tech1/cd1000enus). Inhibited by 75% and 54% by compound **1** (2-amino-3-[(4-methylphenyl)carbonyl]indolizine-1-carboxamide), SAPK2α and FGFR1 were the two most affected human protein kinases, respectively. Compound **2** (imidazo[1,2-β]pyridazine) inhibited human CDK5/p25, TrkA, FGFR1, Lyn, and Rsk1 by at least 89%. Interestingly, the activity of human CamKI kinase that shares 30% amino acid identities with the kinase domain of *Pf*CDPK1 was not affected by any of the four different inhibitors. The two other

compounds had a similar scaffold as compound **2** and were shown to inhibit *Pf*CDPK1 with potencies in the range of 0.45–0.48 μM. They inhibited a few other human protein kinases at
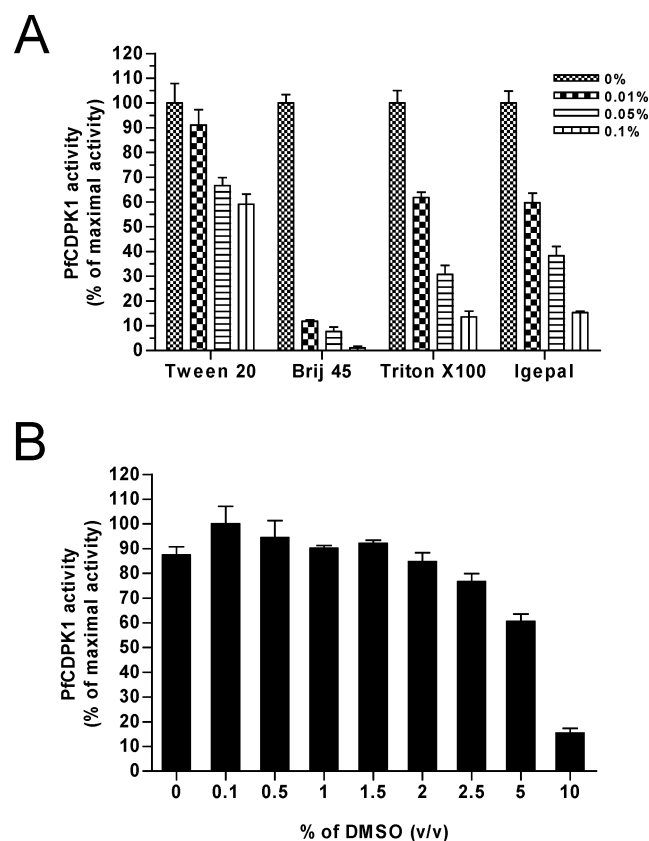

FIGURE 2: Detergent and DMSO tolerance of *Pf*CDPK1. (A) Influence of nonionic surfactant on *Pf*CDPK1 kinase activity. Different concentrations (0.01–0.1%) of Tween 20, Brij 45, Triton X-100, and Igepal were used to assess the sensitivity of *Pf*CDPK1 activity to nonionic detergents. Maximal activity corresponds to the activity in the absence of detergent but in the presence of 10 mM MgCl$_2$, 1 mM CaCl$_2$, 0.5 mM DTT, 0.9 mg/mL β-casein, and 200 μM ATP at pH 7.5. (B) Tolerance of *Pf*CDPK1 to DMSO. *Pf*CDPK1 activity was analyzed in the absence or presence of DMSO (up to 10%) according to assay conditions described in (A).

10 μM (data not shown). While a more complete selectivity study requires available human and plasmodial protein kinases to be tested, the results of this preliminary profiling did not reveal a strong promiscuous behavior of the hit molecules.

Molecular Mode of Inhibition of PfCDPK1. Compound **1** (Figure 4A) was shown to inhibit *Pf*CDPK1 with a submicromolar potency. To assess the mode of inhibition and determine the corresponding kinetic constants, we analyzed the activity of the kinase for increasing concentrations of ATP in the absence or presence of various concentrations of compound **1** (Figure 4). While the maximal velocity fluctuated by a factor less than 1.5 (48 nmol min^{-1} mg^{-1}<V_{max}<72 nmol min^{-1} mg^{-1}), the apparent affinity constant of ATP for the kinase (K_m = 49 μM) increased by more than 6-fold as a function of inhibitor concentration (Figure 4C). With various intersect points at the *X*-axis, the Lineweaver–Burk analysis (Figure 4B) confirmed the ATP-competitive behavior of this chemical series. The constant of inhibition K_i for this inhibitor was calculated from the plot of the different apparent affinity constants (K'_m) as a function of the concentration of the inhibitor. The corresponding ratio *Y*-intercept/slope led to a K_i of 262 nM (Figure 4C). Surface plasmon resonance (SPR) analysis of increasing concentrations of compound **1** was performed on immobilized *Pf*CDPK1 (at the ligand densities described in Experimental Procedures). As shown in Figure 4D, the sensorgrams disclosed a rapid association of the inhibitor and the kinase followed by a rapid dissociation of the complex. The resulting dissociation constant (K_D = k_{off}/k_{on}) was calculated and led to a value of 555 $\pm$ 87 nM (average between spot 1 and spot 2 values, Table 1).

A second chemical series was found to be more potent than series 1. Notably, 11 compounds were identified with IC$_{50}$ values below 100 nM. Compound **2** was the most potent one, exhibiting an IC$_{50}$ value of 9 nM. As for compound **1**, we determined the mode and efficiency of inhibition of compound **2**. The maximal velocity (Figure 5A,C) was found in the range of 50–70 nmol min^{-1} mg^{-1}, confirming the quality and reliability of the enzymatic conditions and thus the consistency of the catalytic constant (K_{cat}). The apparent affinity constant of ATP for the kinase (K_m = 66 μM) was found to increase as a function of inhibitor concentration. Here again, various intersect
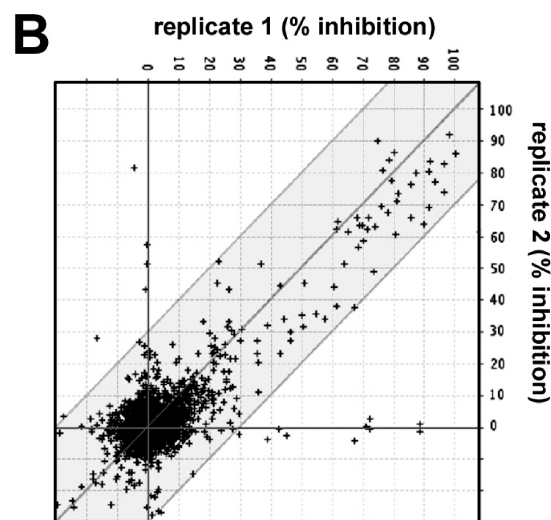

FIGURE 3: Statistical and qualitative analysis of the primary screening results. (A) Statistics of the primary screening campaign. Data were normalized using the GeneData software. Neutral controls represent conditions without inhibitor, and blank controls correspond to conditions without enzyme. (B) Interexperiment reproducibility of the assay in screening conditions. The scatter plot diagram shows the percentage of inhibition of 9878 compounds tested in two independent experiments.
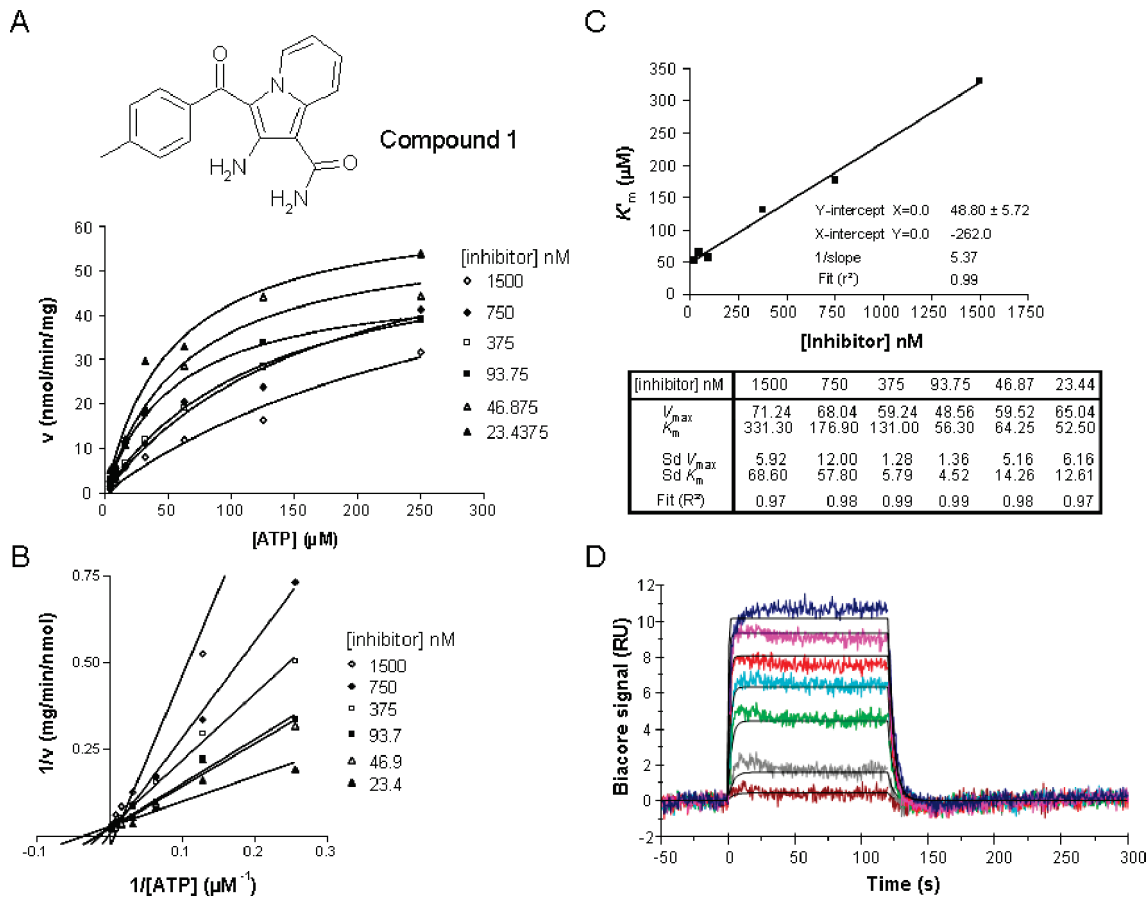
FIGURE 4: Molecular mode of action of compound **1**. (A) Kinetic-based analysis of enzyme inhibition by compound **1** (first series) using Michaelis−Menten graphical representation. Activity of the recombinant enzyme was determined by a radioactive filtration assay. *Pf*CDPK1 was incubated with increasing concentrations of $[\gamma\text{-}^{33}\text{P}]$ATP in the presence of increasing concentrations of compound **1** and 0.9 mg/mL β-casein, 10 mM MgCl$_2$, 1 mM CaCl$_2$, and 0.5 mM DTT at pH 7.5 for 15 min. (B) Lineweaver−Burk representation of results shown in (A). The representation suggests that compound **1** inhibits *Pf*CDPK1 via an ATP competitive mechanism. (C) Determination of the K_i value of compound **1**. Apparent affinity constants (K'_m) are plotted as a function of each corresponding concentration of inhibitor. The K_i value is calculated from the Y-intercept value at $X = 0$ divided by the slope of the linear regression. (D) SPR-based kinetic characterization of compound **1** binding to *Pf*CDPK1. Compound **1** was injected at concentrations above and below the K_D value (10−5000 nM) after immobilization of *Pf*CDPK1. Sensorgrams (in color) and curve fit (black lines) (assuming 1:1 interactions) are shown. K_D values shown in Table 1 were calculated from the association equilibrium data extracted from these sensorgrams.

Table 1: Kinetic Parameters of the Interaction between Small Molecules and *Pf*CDPK1

compd	evaluation	K_D (μM)		k_{on} (1/(M s))		k_{off} (1/s)		χ^2 (RU^2)	
		spot 1	spot 2	spot 1	spot 2	spot 1	spot 2	spot 1	spot 2
1	steady state	0.790	0.507					0.1712	0.1616
	kinetic	0.642	0.468	394300	516300	0.2531	0.2417	0.1569	0.1378
2	steady state	0.106	0.079					0.2344	0.1348
	kinetic	0.073	0.069	378300	441100	0.0275	0.0304	0.2774	0.2847

points with the X-axis of the Lineweaver−Burk analysis confirmed that compound **2** inhibited the kinase in an ATP-competitive manner (Figure 5B). The different apparent affinity constants were plotted as a function of the inhibitor concentration, and the corresponding ratio Y-intercept/slope led to a K_i of 37 nM (Figure 5C). Increasing concentrations of compound **2** were analyzed by SPR on immobilized *Pf*CDPK1 (at the ligand densities described in Experimental Procedures). The resulting sensorgrams revealed a rapid association of the inhibitor and the kinase followed by a dissociation of the complex (Figure 5D), which was slower than the one observed with compound **1**. Here, a dissociation constant ($K_D = k_{off}/k_{on}$) of 71 ± 2 nM was calculated (average between spot 1 and spot 2 values, Table 1).

Molecular Modeling of the Inhibitor−Kinase Complex. Calcium calmodulin-dependent protein kinase of *C. parvum* was found to be the closest protein kinase to *Pf*CDPK1 with known three-dimensional structure. The most important differences in the amino acid sequences of both apicomplexan protein kinases reside in the composition of the actual hinge region (residues 281−285 of the *Cp*CDPK structure; Figure 6A). However, the majority of the differences concern amino acid side chain residues pointing away from the active site and were not considered crucial to the identification of the binding mode. Other residues that are different, but deemed to be conservative changes, include Trp211, Ala234, and Phe248 in *Cp*CDPK which are replaced with Tyr67, Ile84, and Ile113 in *Pf*CDPK1, respectively. The detailed analysis
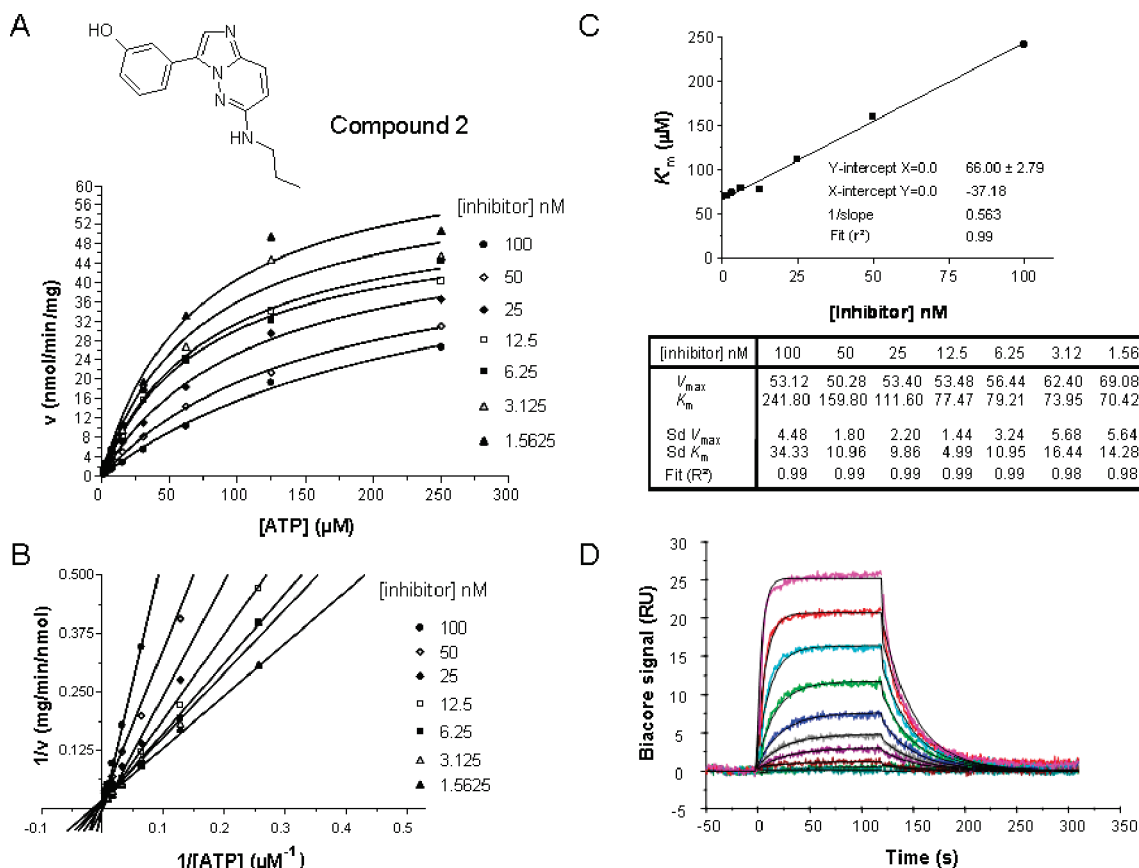
FIGURE 5: Molecular mode of action of compound **2**. (A) Kinetic-based analysis of enzyme inhibition by compound **2** (second series) using the Michaelis−Menten graphical representation. Activity of the recombinant enzyme was determined as described for Figure 4 and in the presence of increasing concentrations of compound **2**. (B) Lineweaver−Burk representation of results shown in (A). The representation suggests that compound **2** inhibits PfCDPK1 according to an ATP competitive mechanism. (C) Determination of the K_i value of compound **2**. Apparent affinity constants (K'_m) are plotted as a function of each corresponding concentration of inhibitor. The K_i value is calculated from the Y-intercept value at $X = 0$ divided by the slope of the linear regression. (D) SPR-based kinetic characterization of compound **2** binding to PfCDPK1. Compound **2** was injected at concentrations above and below the K_D value (10−5000 nM) after immobilization of PfCDPK1. Sensorgrams (in color) and curve fit (black lines) (assuming 1:1 interactions) are shown. K_D values shown in Table 1 were calculated from the association equilibrium data extracted from these sensorgrams.

of the interaction parameters of both series of inhibitors led to a major difference: The residence time of compound **2** when bound to PfCDPK1 is 1 order of magnitude higher than that of compound **1** while the association rate is not significantly different (1.1-fold). The proposed binding mode of the two small molecules, as determined by the docking experiments into the close analogue of the PfCDPK1 active site, was hence examined in the hope of explaining these differences. Compound **1** is predicted to bind to CpCDPK (and thus also PfCDPK1) through the formation of two hydrogen bonds between the target protein (main chain carbonyl oxygen of Glu281 and the main chain amide nitrogen of Cys283) and the amide moiety of compound **1** (Figure 6B). While the pose do satisfy the minimum required interaction (the formation of this hydrogen bond interaction with the proton-donating peptide bond of Glu281), there are no other satisfying interactions with the protein. Notably, the contribution to binding of hydrophobic interactions within the resulting complex of compound **1** with the protein is extremely low (−1.9 kcal/mol), especially when compared with the hydrophobic component of other small molecule inhibitors into the same binding pocket (−2.45 kcal/mol for staurosporine). The overall docking score (using the Glide overall scoring function Gscore) is very low (−2.3) when compared with that of the reference molecule staurosporine (−8.3). The small molecule would also appear to have a pose in which the majority of the hydrophobic core is

exposed to the solvent, as opposed to fitting well within the groove of the binding pocket.

The predicted binding pose of compound **2** would appear to be superior for several reasons. This compound also would form a hydrogen interaction between the hinge region protein donor and the phenol moiety of the small molecule. However, a second hydrogen bond interaction is predicted between the secondary amine and the main chain carbonyl of Ile346 (Figure 6C). The fact that there are two hydrogen bonds predicted at opposite ends of the small molecule would tend to support its higher affinity. The overall complementarity of the fit and the higher contribution of hydrophobic interactions would also tend to confirm the superiority of compound **2** (data not shown).

Aiming at better understanding the structural requirements that govern the interaction between small molecules and PfCDPK1, we determined the potency of close analogues of compound **2**, and the results were analyzed in view of the sterical constraints hypothesized from the predictive 3D modeling of the kinase's ATP-binding pocket.

The nature and the position of scaffold decorations can dramatically modify potency of compound **2**. As seen in Table 2, the replacement of the hydroxyl group by a fluoro acceptor group led to a 50-fold decrease of the potency (entry 2). The fact that the proton-donating hydroxyl group could be replaced by a putative proton acceptor such as a fluoro group prompted us to examine
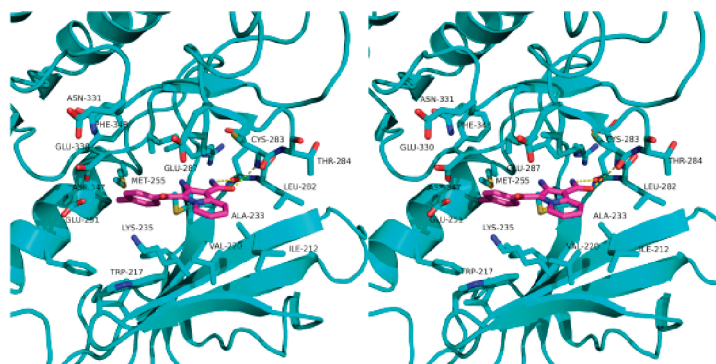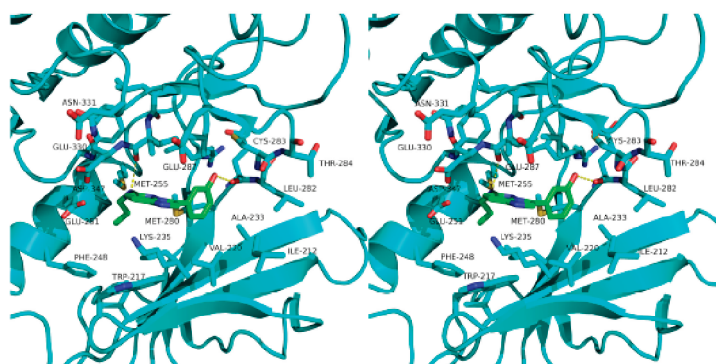
A

B

C

FIGURE 6: Molecular modeling of the small molecule inhibitor−kinase complex. The sequence of the core domain of *Pf*CDPK1 including residues 47−346 was aligned with the region of the *C. parvum* calcium calmodulin-dependent protein kinase, which corresponds to residues 197−457. An overall sequence identity of 37% was calculated (A). Compound **1** (B) and compound **2** (C) are shown in magenta and green, respectively. They were docked into the ATP binding site of the α carbon chain modeled structure of the *C. parvum* calcium calmodulin-dependent protein kinase. For compound **2**, out of the hydrogen interaction between the hinge region protein donor and the phenol moiety of the small molecule, a second hydrogen bond interaction is predicted between the secondary amine and the main chain carbonyl of Ile346.

the possible binding mode of other analogues. The addition of a methoxy (entry 3) or methyl (entry 4) group in the ortho position completely abolished the potency. However, the replacement of the hydroxyl group by other H-bond acceptor groups, such as 3,4-methylenedioxy (entry 5), was tolerated and maintained significant potency. Interestingly, the 4-hydroxy-3-methoxy-substituted compound (entry 6) exhibited a nanomolar range IC_{50} value close to the one of compound **2**. Other H-bond donor groups can be tolerated, like the carboxyl group, except that in this case the para-substituted compound (entry 7) was significantly more active than the meta-substituted analogue (entry 8).

DISCUSSION

In the present study, we conducted a primary screening campaign of 54700 small molecules aimed at identifying potent inhibitors of *Pf*CDPK1. Subsequently to their confirmation, hit compounds were used as molecular tools to better define the

structural parameters of the inhibition and to anticipate the design of novel inhibitors. Two different chemical series have been identified, and molecules of both series were shown to be ATP-competitive inhibitors.

The validity of the results generated by a molecular screening of several thousand small molecules relies in part on the quality of the purified protein target. In the case of *Pf*CDPK1, the confirmation of the catalytic activity and the kinetic parameters of the kinase when compared to published data was critical prior to initiating the screening process. To date, too few proteins have been identified and ultimately proposed as possible physiological substrates of *Pf* CDPK1, and therefore, no consensus amino acid sequence is available to characterize the phosphorylation site. The choice among various substrate molecules that could have been used in the course of primary screening was motivated by the notion that protein substrates are more prone than peptidic substrates to reflect the structural requirements that the overall

Table 2: Potency of Compound **2** Analogues

Entry	Compound	Group(s) tested	IC50 (μM)
1	2	OH	0.009
2	3	F	0.464
3	4	MeO,	19.1
4	5	Me, F	> 20
5	6		0.078
6	7	OH, OMe	0.022
7	8	CO_2H	0.167
8	9	CO_2H	2.0

protein conformation inflicts to a protein kinase during catalysis. Indeed, the catalytic activity of human protein kinases like casein kinase 2 (CK2) was found to be stimulated efficiently by effectors exclusively when proteins were used as substrates (*36*). The phosphoinositide-dependent protein kinase 1 is another example of a protein kinase which has the property of sensing the conformation of its protein substrates (*37*). Regulatory subunits are also responsible for long-distance effects that influence substrate recognition and kinase activation (*38, 39*). The identification of *Pf*CDPK1 protein substrates with physiological relevance is crucial to better understand the regulation of and the role played by this particular kinase within *Plasmodium*. Recently, some studies pointed out potential *in vivo* protein substrates of *Pf*CDPK1. First, *Pf*PE-PB1, the plasmodial Raf kinase inhibitory protein (RKIP), has been shown to be phosphorylated by and to stimulate the autophosphorylation of *Pf*CDPK1 (5-fold increase), which consequently inhibited the phosphorylation of exogenous substrates (*40*). Second, the myosin A tail domain–interacting protein (MTIP) and the glideosome-associated protein 45 (GAP45), two components of the parasite motor complex, have been found phosphorylated by *Pf*CDPK1 *in vitro* (*31*) and *in vivo* (*41*). This observation suggested that *Pf*CDPK1 could exert a putative regulation of myosin function in the process of parasite motility.

Consequently to the development of a robust assay, compounds tested in duplicate resulted in a very good correlation following two independent analyses. However, the limitation of the technology was linked to the use of a low micromolar concentration of ATP. Since the consequence of screening small molecules at a concentration of ATP which is lower than its K_m is the overestimation of their potency, screening results were confirmed by the use of a radioactive filtration assay. Accordingly, the K_i values of the two compounds representative of the main chemical series newly identified were found to be 4-fold higher than the corresponding IC$_{50}$ values determined in the ATP-consumption format. The concentration of ATP in the assay is not the only parameter that needed to be considered. Notably, a short reaction time was more suitable to satisfy Michaelis–Menten conditions during K_i determination as compared to IC$_{50}$ evaluation.

The evolution of both the maximal velocity and the apparent affinity of ATP for *Pf*CDPK1 with increasing concentrations of

small molecules demonstrated that both inhibitors had a clear negative impact on the binding of ATP but not on the catalytic constant. ATP-competitive behavior is a common mechanism of action for many protein kinase inhibitors. Recently, the inhibition of *Pf*CDPK1 by 2,6,9-trisubstituted purines was shown to lead to a rapid arrest of schizont development in *P. falciparum* (*31*). Similarly to this study, we found inhibitors whose potency against *Pf*CDPK1 translated into a decrease of parasite proliferation while other molecules did not exhibit any correlation between both assays. For instance, one of the most potent imidazopyridazine compounds (compound **2** series), displayed an IC$_{50}$ of 10 nM in the enzymatic assay and an EC$_{50}$ of 5.7 μM when tested on live *P. falciparum*, whereas another molecule of the same chemical series was found to inhibit *Pf*CDPK1 and parasite growth with potencies of 90 nM and 1.5 μM, respectively. Such a discrepancy between molecular and phenotypic screenings is a common feature of molecules tested for potential antimalarial properties and is mainly due to a large variability in their capacity to cross several cellular membranes. In a culture system such as a mix of live parasites and red blood cells, the ability of any inhibitor to penetrate the erythrocytic plasma membrane represents the first barrier to overcome. Then, the membrane of the parasite needs to be crossed by the small molecule and thus represents the second limiting step. Additional hurdles such as plasma/serum proteins that bind the inhibitor and sequester it out of its site of action can also explain why potent molecules against purified enzyme turn out to be poor inhibitors when tested in cell culture conditions. The study published by Kato and co-workers (*31*) has clearly shown that a pharmacological inhibition of *Pf*CDPK1 might lead to parasite growth limitation, validating this target and some of its inhibitors as potential starting points for a therapeutic approach. In other words, potent inhibitors reaching intracellular *Pf*CDPK1 translate systematically into a decrease of intraerythrocytic parasitemia.

Here, we aimed at defining parameters governing target–inhibitor interaction and that could help to better derive new small molecule scaffolds with increased potency, higher specificity, and better efficacy. We anticipated that improving the stability of the inhibitor–kinase complex could be beneficial for the efficacy of new molecules exhibiting low plasma protein binding, when tested on live parasites. While exhibiting the same molecular mechanism of action, compound **1** (2-amino-3-[(4-methylphenyl) carbonyl]indolizine-1-carboxamide) and compound **2** (imidazo [1,2-β]pyridazine) differ through the fact that the latter one has an extended time of interaction with the kinase. Association constants of both compounds have been calculated in the range of 4.0×10^5–4.6×10^5 M^{-1} s^{-1}. These values are much lower than k_+, the transport rate constant between a small molecule and its protein binding site in solution, indicating that binding of both compounds is not diffusion-limited (*42*). Moreover, our observation of compound **2** properties is in good agreement with a lower dissociation rate, a lower inhibition constant, and a better stability into the ATP-binding pocket of the kinase. Indeed, confirmed by homology-based modeling, key interactions were highlighted between specific amino acid residues of this pocket and structurally well-positioned atoms of the small molecules. To date, no tertiary structure has been reported for *Pf*CDPK1 or for any closely related plasmodial kinase, and the homology-based model of the kinase core domain was the only predicted structural information we were relying on for the docking of small molecules. Aware of this limitation and of the possibility that the hypothesized structural constraints could be misevaluated, we

worked with a high degree of flexibility of the α carbon chain. In addition, we evaluated the quality of the fit and the stability of the complex upon energy minimization steps. While not being an absolute demonstration of the structural parameters that govern the interaction between various small molecules and the kinase, the model offers the possibility of shedding light on potential key amino acid residues that need to be considered in the design of new molecules. The compilation of results generated by new decorations of the main scaffolds will in turn feed the refining of the modeled structure. Indeed, the amino acid residues and the atoms of the molecules that appear to be crucial for a prolonged residence time of the inhibitor in its binding site will be considered as important parameters to guide the design of the SAR and the synthesis of new small molecules.

ACKNOWLEDGMENT

REFERENCES

1. White, N. J. (2004) Antimalarial drug resistance. *J. Clin. Invest. 113*, 1084–1092.
2. Uhlemann, A. C., Yuthavong, Y., and Fidock, D. (2005) Mechanisms of antimalarial drug action and resistance, in Molecular Approaches to Malaria (Sherman I. W., Ed.) pp 229−261, ASM Press, Washington, DC.
3. Enosse, S., Magnussen, P., Abacassamo, F., Gómez-Olivé, X., Rønn, A. M., Thompson, R., and Alifrangis, M. (2008) Rapid increase of *Plasmodium falciparum* dhfr/dhps resistant haplotypes, after the adoption of sulphadoxine-pyrimethamine as first line treatment in 2002, in southern Mozambique. *Malar. J. J7*, 115.
4. Saito-Nakano, Y., Tanabe, K., Kamei, K., Iwagami, M., Komaki-Yasuda, K., Kawazu, S., Kano, S., Ohmae, H., and Endo, T. (2008) Genetic evidence for *Plasmodium falciparum* resistance to chloroquine and pyrimethamine in Indochina and the Western Pacific between 1984 and 1998. *Am. J. Trop. Med. Hyg. 79*, 613–619.
5. Zhong, D., Afrane, Y., Githeko, A., Cui, L., Menge, D. M., and Yan, G. (2008) Molecular epidemiology of drug-resistant malaria in western Kenya highlands. *BMC Infect. Dis. 8*, 105.
6. White, N. J. (2008) Qinghaosu (artemisinin): the price of success. *Science 320*, 330–334.
7. Doerig, C., Billker, O., Haystead, T., Sharma, P., Tobin, A. B., and Waters, N. C. (2008) Protein kinases of malaria parasites: an update. *Trends Parasitol. 24*, 570–577.
8. Leroy, D., and Doerig, C. (2008) Drugging the *Plasmodium* kinome: the benefits of academia-industry synergy. *Trends Pharmacol. Sci. 29*, 241–249.
9. Doerig, C., and Meijer, L. (2007) Antimalarial drug discovery: targeting protein kinases. *Expert Opin. Ther. Targets 11*, 279–290.
10. Doerig, C., Billker, O., Pratt, D., and Endicott, J. (2005) Protein kinases as targets for antimalarial intervention: Kinomics, structure-based design, transmission-blockade, and targeting host cell enzymes. *Biochim. Biophys. Acta 1754*, 132–150.
11. Geyer, J. A., Prigge, S. T., and Waters, N. C. (2005) Targeting malaria with specific CDK inhibitors. *Biochim. Biophys. Acta 1754*, 160–170.
12. Vaid, A., Thomas, D. C., and Sharma, P. (2008) Role of Ca^{2+}/calmodulin-PfPKB signaling pathway in erythrocyte invasion by *Plasmodium falciparum*. *J. Biol. Chem. 283*, 5589–5597.
13. McRobert, L., Taylor, C. J., Deng, W., Fivelman, Q. L., Cummings, R. M., Polley, S. D., Billker, O., and Baker, D. A. (2008) Gametogenesis in malaria parasites is mediated by the cGMP-dependent protein kinase. *PLoS Biol. 6* (6), e139.
14. Rangarajan, R., Bei, A., Henry, N., Madamet, M., Parzy, D., Nivez, M. P., Doerig, C., and Sultan, A. (2006) Pbcrk-1, the *Plasmodium berghei* orthologue of P. falciparum cdc-2 related kinase-1 (Pfcrk-1), is essential for completion of the intraerythrocytic asexual cycle. *Exp. Parasitol. 112*, 202–207.
15. Rangarajan, R., Bei, A. K., Jethwaney, D., Maldonado, P., Dorin, D., Sultan, A. A., and Doerig, C. (2005) A mitogen-activated protein kinase regulates male gametogenesis and transmission of the malaria parasite *Plasmodium berghei*. *EMBO Rep. 6*, 464–469.
16. Spry, C., Chai, C. L., Kirk, K., and Saliba, K. J. (2005) A class of pantothenic acid analogs inhibits *Plasmodium falciparum* pantothenate kinase and represses the proliferation of malaria parasites. *Antimicrob. Agents Chemother. 49*, 4649–4657.
17. Spry, C., Kirk, K., and Saliba, K. J. (2008) Coenzyme A biosynthesis: an antimicrobial drug target. *FEMS Microbiol. Rev. 32*, 56–106.
18. Dorin-Semblat, D., Sicard, A., Doerig, C., Ranford-Cartwright, L., and Doerig, C. (2008) Disruption of the *Pf*PK7 gene impairs schizogony and sporogony in the human malaria parasite *Plasmodium falciparum*. *Eukaryot. Cell 7*, 279–285.
19. Dorin-Semblat, D., Quashie, N., Halbert, J., Sicard, A., Doerig, C., Peat, E., Ranford-Cartwright, L., and Doerig, C. (2007) Functional characterization of both MAP kinases of the human malaria parasite *Plasmodium falciparum* by reverse genetics. *Mol. Microbiol. 65*, 1170–1180.
20. Reininger, L., Billker, O., Tewari, R., Mukhopadhyay, A., Fennell, C., Dorin-Semblat, D., Doerig, C., Goldring, D., Harmse, L., Ranford-Cartwright, L., Packer, J., and Doerig, C. (2005) A NIMA-related protein kinase is essential for completion of the sexual cycle of malaria parasites. *J. Biol. Chem. 280*, 31957–31964.
21. Tewari, R., Dorin, D., Moon, R., Doerig, C., and Billker, O. (2005) An atypical mitogen-activated protein kinase controls cytokinesis and flagellar motility during male gamete formation in a malaria parasite. *Mol. Microbiol. 58*, 1253–1263.
22. Harper, J. F., and Harmon, A. (2005) Plants, symbiosis and parasites: a calcium signalling connection. *Nat. Rev. Mol. Cell. Biol. 6*, 555–566.
23. Zhao, Y., Kappes, B., and Franklin, R. M. (1993) Gene structure and expression of an unusual protein kinase from *Plasmodium falciparum* homologous at its carboxyl terminus with the EF hand calcium-binding proteins. *J. Biol. Chem. 268*, 4347–4354.
24. Farber, P. M., Graeser, R., Franklin, R. M., and Kappes, B. (1997) Molecular cloning and characterization of a second calcium-dependent protein kinase of *Plasmodium falciparum*. *Mol. Biochem. Parasitol. 87*, 211–216.
25. Li, J. L., Baker, D. A., and Cox, L. S. (2000) Sexual stage-specific expression of a third calcium-dependent protein kinase from *Plasmodium falciparum*. *Biochim. Biophys. Acta 1491*, 341–349.
26. Billker, O., Dechamps, S., Tewari, R., Wenig, G., Franke-Fayard, B., and Brinkmann, V. (2004) Calcium and a calcium-dependent protein kinase regulate gamete formation and mosquito transmission in a malaria parasite. *Cell 117*, 503–514.
27. Ward, P., Equinet, L., Packer, J., Doerig, C., and Protein (2004) kinases of the human malaria parasite *Plasmodium falciparum*: the kinome of a divergent eukaryote. *BMC Genomics 5*, 79.
28. Zhao, Y., Pokutta, S., Maurer, P., Lindt, M., Franklin, R. M., and Kappes, B. (1994) Calcium-binding properties of a calcium-dependent protein kinase from *Plasmodium falciparum* and the significance of individual calcium-binding sites for kinase activation. *Biochemistry 33*, 3714–3721.
29. Zhao, Y., Franklin, R. M., and Kappes, B. (1994) *Plasmodium falciparum* calcium-dependent protein kinase phosphorylates proteins of the host erythrocytic membrane. *Mol. Biochem. Parasitol. 66*, 329–343.
30. Möskes, C., Burghaus, P. A., Wernli, B., Sauder, U., Durrenberger, M., and Kappes, B. (2004) Export of *Plasmodium falciparum* calcium-dependent protein kinase 1 to the parasitophorous vacuole is dependent on three N-terminal membrane anchor motifs. *Mol. Microbiol. 54*, 676–691.
31. Kato, N., Sakata, T., Breton, G., Le Roch, K. G., Nagle, A., Andersen, C., Bursulaya, B., Henson, K., Johnson, J., Kumar, K. A., Marr, F., Mason, D., McNamara, C., Plouffe, D., Ramachandran, V., Spooner, M., Tuntland, T., Zhou, Y., Peters, E. C., Chatterjee, A., Schultz, P. G., Ward, G. E., Gray, N., Harper, J., and Winzeler, E. A. (2008) Gene expression signatures and small-molecule compounds link a protein kinase to *Plasmodium falciparum* motility. *Nat. Chem. Biol. 4*, 347–356.
32. Zhang, J. H., Chung, T. D., and Oldenburg, K. R. (1999) "A simple statistical parameter for use in evaluation and validation of high throughput screening assays". *J. Biomol. Screen. 4*, 67–73.
33. Myszka, D. G. (2004) Analysis of small-molecule interactions using Biacore S51 technology. *Anal. Biochem. 329*, 316–323.
34. Friesner, R. A., Banks, J. L., Murphy, R. B., Halgren, T. A., Klicic, J. J., Mainz, D. T., Repasky, M. P., Knoll, E. H., Shelley, M., Perry, J. K., Shaw, D. E., Francis, P., and Shenkin, P. S. (2004) Glide: a new

approach for rapid, accurate docking and scoring. 1. Method and assessment of docking accuracy. *J. Med. Chem. 47*, 1739–1749.

35. Pomel, V., Klicic, J., Covini, D., Church, D. D., Shaw, J. P., Roulin, K., Burgat-Charvillon, F., Valognes, D., Camps, M., Chabert, C., Gillieron, C., Françon, B., Perrin, D., Leroy, D., Gretener, D., Nichols, A., Vitte, P. A., Carboni, S., Rommel, C., Schwarz, M. K., and Ruckle, T. (2006) Furan-2-ylmethylene thiazolidinediones as novel, potent, and selective inhibitors of phosphoinositide 3-kinase γ. *J. Med. Chem. 49*, 3857–3871.

36. Leroy, D., Heriché, J.-K., Filhol, O., Chambaz, E. M., and Cochet, C. (1997) Binding of polyamines to an autonomous domain of the regulatory subunit of protein kinase CK2 induces a conformational change in the holoenzyme. A proposed role for the kinase stimulation. *J. Biol. Chem. 272*, 20820–20827.

37. Biondi, R. M. (2004) Phosphoinositide-dependent protein kinase 1, a sensor of protein conformation. *Trends Biochem. Sci. 29*, 136–142.

38. Ubersax, J. A., and Ferrell, J. F., Jr. (2007) Mechanisms of specificity in protein phosphorylation. *Nat. Rev. Molecular Cell Biol. 8*, 530–541.

39. Loog, M., and Morgan, D. O. (2005) Cyclin specificity in the phosphorylation of cyclin-dependent kinase substrates. *Nature 434*, 34–35.

40. Kugelstadt, D., Winter, D., Pluckhahn, K., Lehmann, W. D., and Kappes, B. (2007) Raf kinase inhibitor protein affects activity of *Plasmodium falciparum* calcium-dependent protein kinase 1. *Mol. Biochem. Parasitol. 151*, 111–117.

41. Green, J. L., Rees-Channer, R. R., Howell, S. A., Martin, S. R., Knuepfer, E., Taylor, H. M., Grainger, M., and Holder, A. A. (2008) The motor complex of *Plasmodium falciparum*: Phosphorylation by a calcium-dependent protein kinase. *J. Biol. Chem. 283*, 30980–30989.

42. Lauffenburger, D. A., and Linderman, J. J. (1996) Receptors: Models for binding, Trafficking and Signaling , pp 146−147, Oxford University Press, Cary, NC.